

Yousef Hakim

Dr. Chetan Patil, Dr. Michel Lemay

Honors Scholars Project

## Paving the Road for Coherent Anti-Stokes Raman Scattering (CARS)

### Imaging of Myelin

#### Table of Contents

Abstract.....	3
Introduction .....	4
Demyelination .....	4
Helper T Cells .....	6
Cytotoxic T Cells .....	6
Autoreactive T Cells .....	6
Microglia and Macrophages .....	7
B Cells.....	7
Impaired Proteolytic Activity .....	7
Remyelination.....	8
Steps of Remyelination .....	9
Models and Approaches to Study Demyelination and Remyelination.....	10
In Vitro Models .....	11
Ex Vivo Models .....	12
In Vivo Models.....	13
Results of Studies of Demyelination and Remyelination.....	15
Demyelination .....	15
Remyelination .....	16
Unknowns about Demyelination and Remyelination.....	17
Demyelination .....	17
Remyelination .....	18
Microscopic and Spectroscopic Methods Used to Detect the Myelin.....	18

Fluorescence Microscopy .....	19
Multiphoton Microscopy .....	20
Spatially Offset Raman Spectroscopy (SORS) .....	20
Near Infrared (NIR) Spectroscopy .....	20
Project Overview.....	21
Methods.....	22
Imaging of Engineered Adipose Tissue.....	22
Image Analysis in ImageJ .....	22
Design and Construction of a Mini Incubation Chamber .....	23
Developing a Procedure for Demyelination .....	26
Results.....	26
Imaging of Engineered Adipose Tissue.....	26
Image Analysis in ImageJ .....	27
Construction of a Mini Incubation Chamber .....	33
Developing a Procedure for Demyelination .....	37
Discussion .....	38
Imaging of Engineered Adipose Tissue.....	38
Image Analysis in ImageJ .....	38
Construction of a Mini Incubation Chamber .....	39
Developing a Procedure for Demyelination .....	39
Conclusion.....	40
Acknowledgements.....	40
References .....	40

## Abstract

Demyelinating diseases, such as multiple sclerosis (MS), result in the deterioration of the myelin sheath that covers the neural cells of the brain. A microscopy method that can be used to assess the effectiveness of therapeutics aimed at healing demyelinating diseases and to further study these diseases is needed. Specifically, a microscopy method with high specificity to myelin and low photobleaching of myelin is needed. Photobleaching is the fading of fluorescence after repeated cycles of excitation. Currently, fluorescence microscopy and similar methods that result in photobleaching and use dyes have been used to visualize the myelin. Dyes, however, stain tissue samples and may affect molecular functions. Besides these methods, coherent anti-Stokes Raman scattering (CARS) microscopy has also been used. In contrast to other used microscopy methods, CARS microscopy's photobleaching can be minimized, and CARS microscopy does not use stains.

As an initial step toward investigating the ability of the CARS microscope to visualize different levels of myelin, which consists primarily of lipids, and to demonstrate CARS value for use in studying demyelinating diseases and in the development of therapeutic efficacy of drugs developed to treat MS; CARS imaging of lipid droplets in engineered adipose tissue was performed, and quantification and measurement of the lipid droplets was done. In addition, a mini incubation chamber for long-term *in vitro* imaging of demyelination was built, and a protocol for a demyelination study has been developed.

## Introduction

### Demyelination

The myelin sheath is a membrane that insulates the axons, allowing for quick propagation of electrical signals between neurons (Singh & Sarma, 2016). In the central nervous system (CNS), the myelin sheath is formed by glial cells called oligodendrocytes, which extend their processes around the axons and wrap axons in myelin (Olsen & Akirav, 2015). During demyelination, this myelin sheath degenerates, affecting the propagation of the electrical signal and, thus, disrupting the communication between neurons (Singh & Sarma, 2016). Demyelination can be caused by genetic, environmental, viral, or immunological factors, and it occurs in neurological diseases, such as multiple sclerosis (MS) that affects the brain and the spinal cord, neuromyelitis optica that affects the optic nerve and the spinal cord, and acute disseminated encephalomyelitis that affects the brain and the spinal cord (Singh & Sarma, 2016). Some of the symptoms of these diseases are muscle weakness and loss of coordination. Among these diseases, MS is the most studied (Singh & Sarma, 2016). Hence, MS will be used to explain how demyelination occurs.

MS is mediated by two *possibly* independent events: inflammation, which results in the formation of white matter lesions, and neurodegeneration, which results in brain damage (Singh & Sarma, 2016). After inflammation results in the formation of white matter lesions, these lesions are characterized by further inflammation, primary demyelination, and astrocytic scar formation (Singh & Sarma, 2016). Primary demyelination is demyelination that results from attacks on oligodendrocytes (Franklin, 2008). Regarding astrocytic scar formation, these scars are formed by reactive

astrocytes, a type of glial cells. These cells release molecules that promote inflammation, and their processes form a dense network, resulting in a scar formation (Gallo & Armstrong, 2008). Glial scars inhibit regeneration and OPC migration, which will be discussed later (Gallo & Armstrong, 2008).

Neurodegeneration results in oligodendrocytes' apoptosis, or death; and axonal degeneration promotes neurodegeneration (Singh & Sarma, 2016; Franklin, 2008).

Neurodegeneration that exists before the beginning of the disease amplifies the damage that occurs (Singh & Sarma, 2016). The reason behind this occurrence is that neurodegeneration results in the activation of microglia, which are involved in removal of tissue debris (Singh & Sarma, 2016). These microglia can easily become effector cells that attack other cells in response to proinflammatory molecules (Singh & Sarma, 2016). In other words, if microglia are activated before the beginning of the disease, they can easily become effector cells when the disease results in inflammation, making the body more susceptible to damage due to inflammation (Singh & Sarma, 2016).

In sum, MS is mediated by two events: inflammation and neurodegeneration (Singh & Sarma, 2016). Preexisting neurodegeneration also makes the body more susceptible to inflammation-caused damage.

Of the two events (inflammation and neurodegeneration), inflammation is the primary event that results in subsequent injury in MS (Singh & Sarma, 2016). In fact, inflammation plays a role in all MS lesions (Singh & Sarma, 2016). In this inflammatory response, helper T cells, cytotoxic T cells, autoreactive T cells, microglia and macrophages, B cells, and impaired proteolytic activity play a role in causing demyelination.

### *Helper T Cells*

A type of helper T cells has been identified as having an important role in MS. This type of helper T cells is called Th17 (Singh & Sarma, 2016). Th17 activate in response to molecules produced by their antigens, the molecules to which they bind (Singh & Sarma, 2016). When activated, helper T cells activate cytotoxic T cells to kill cells that present this antigen, order B cells to produce antibodies against the antigen-presenting cells, and result in macrophages' destruction of the cells (Alberts et al., 2002). Th17 cells also activate other Th17 cells by secreting molecules (Singh & Sarma, 2016). Th17 can be inhibited by Treg cells, which are anti-inflammatory T cells (Singh & Sarma, 2016).

### *Cytotoxic T Cells*

Once activated by helper T cells, cytotoxic T cells kill the cells that present the antigen that activated the helper T cells (Alberts et al., 2002). In demyelination, cytotoxic T cells can kill oligodendrocytes and neurons by recognizing their antigens (Singh & Sarma, 2016). Cytotoxic T cells can also kill neurons by an antigen-independent mechanism, which involves a death receptor present in demyelinating lesions (Singh & Sarma, 2016).

### *Autoreactive T Cells*

Autoreactive T cells are T cells that are specific to the antigens of the cells of the body (Pette et al., 1990). For example, there are T cells specific to the myelin basic protein (MBP), which is present in the myelin sheath of neurons (Pette et al., 1990). In fact, MBP is considered an antigen in MS lesions (Singh & Sarma, 2016). That is, MBP-

presenting cells are attacked by the body's immune system in MS. Interestingly, autoreactive T cells are also present in healthy individuals (Singh & Sarma, 2016). Further, autoreactive T cells have CD4+ and CD8+ T cell phenotypes, meaning they can be helper T cells or cytotoxic T cells, respectively (Singh & Sarma, 2016). Both of these T cell types induce inflammation and autoimmunity, which is the immune system's attack on the body itself (Singh & Sarma, 2016).

### *Microglia and Macrophages*

Microglia and macrophages remove tissue debris, and they are derived from circulating monocytes, a type of blood cells that passes through the blood brain barrier (BBB), and from local microglia in the brain (Singh & Sarma, 2016). In MS, these cells release molecules that are involved in tissue injury and phagocytosis, the ingestion of cells and molecules (Singh & Sarma, 2016). Macrophages also induce demyelination and axonal injury (Singh & Sarma, 2016).

### *B Cells*

B cells produce antibodies when activated by helper T cells (Alberts et al., 2002). In MS, B cells produce molecules that play a role in the proinflammatory environment of the disease (Singh & Sarma, 2016). Elimination of B cells in MS patients is a form of therapy (Singh & Sarma, 2016).

### *Impaired Proteolytic Activity*

In MS, plasmin activator inhibitor (PAI-1) inhibits the activity of plasmin activator, indicating the inhibition of the proteolytic activity of the plasmin activator (Singh & Sarma, 2016). The inhibition of this proteolytic activity affects the normal functions of

neurons or results in the activation of microglia, which result in axonal injury as mentioned above (Singh & Sarma, 2016).

### Remyelination

When demyelination occurs, the body can start remyelination. Remyelination is the redevelopment of the myelin sheath (Olsen & Akirav, 2015). Remyelination protects the axons from further degeneration and restores normal propagation of electrical signals (Olsen & Akirav, 2015; Goldschmidt, Antel, Konig, Bruck, & Kuhlmann, 2009).

Remyelination, however, does not always occur. If remyelination does not occur or is inefficient, the axons are left unprotected, leading to their degeneration (Franklin, 2008).

Remyelination occurs when the damage to the axons and the myelin sheath is transient, cholesterol production in the CNS is functioning properly, and during early cycles of demyelination/remyelination (Singh & Sarma, 2016; Olsen & Akirav, 2015; Franklin, 2008). Remyelination becomes less effective after repeated cycles of demyelination/remyelination (Franklin, 2008). Remyelination also occurs frequently in acute MS lesions and in chronic lesions (Goldschmidt et al., 2009). Studies provided different results regarding remyelination in chronic lesions. Older studies indicated extensive remyelination in 20% of chronic lesions, whereas a more recent study indicated that remyelination occurs in 60% of chronic lesions (Goldschmidt et al., 2009). However, remyelination does not always result in complete remyelination in lesions, and the location of the lesion plays a role in whether remyelination will occur or not (Goldschmidt et al., 2009).

Remyelination, as mentioned above, does not always occur; and there are challenges for its occurrence. Remyelination rarely occurs in dystrophic axons and is limited in

progressive MS, a type of MS (Franklin, 2008; Olsen & Akirav, 2015). Further, the differentiation of oligodendrocyte progenitor cells (OPC) is a challenge for the occurrence of remyelination. OPC differentiation is a major event in remyelination, and it will be discussed later (Olsen & Akirav, 2015). Nonetheless, in MS lesions, some OPCs remain undifferentiated, posing a challenge for remyelination (Olsen & Akirav, 2015).

### *Steps of Remyelination*

There are two steps for remyelination: differentiation and migration and myelin production. These steps are straightforward. However, there are many unknowns regarding remyelination and demyelination.

### *Differentiation and Migration*

When demyelination occurs and remyelination begins, neural stem cells (NSCs) in the brain are induced by certain signals to differentiate into OPCs (Olsen & Akirav, 2015). For example, NSCs can become OPCs after they overexpress bHLH transcription factor *Ascl1* (Franklin & Gallo, 2014). After that, OPCs need to migrate to the demyelinated area and differentiate into mature oligodendrocytes that can myelinate the axons (Olsen & Akirav, 2015). There are three stages (early-stage cells, preoligodendrocytes, and immature oligodendrocytes) before becoming mature oligodendrocytes (Olsen & Akirav, 2015). Each of the stages can be identified by specific markers that have complementary antibodies. The early-stage cells are identified by A2B5 ganglioside and NG2 proteoglycan (Olsen & Akirav, 2015). The second stage, which is the preoligodendrocyte stage, can be identified by expression of O4 sulfatide (Olsen & Akirav, 2015). The third stage, which is the immature oligodendrocyte stage, can be

identified by the presence of galactosylceramides and O4 and the absence of A2B5 and NG2 (Olsen & Akirav, 2015). Finally, the OPCs become mature oligodendrocytes, which can be identified by multiple molecules, such as myelin basic protein (MBP), myelin associated glycoprotein (MAG), and myelin oligodendrocyte glycoprotein (MOG) (Olsen & Akirav, 2015). These markers are essential in studies of demyelination and remyelination that use OPCs.

### Myelin Production

After the OPCs mature to oligodendrocytes, they start the myelin production step of remyelination. OPCs that migrated to the demyelinated area and matured are not the only cells that result in remyelination. In addition to migrating OPCs, local OPCs at the area of injury also contribute to remyelination (Olsen & Akirav, 2015). Further, in this step of remyelination, the oligodendrocytes extend processes from their cell body, and these processes wrap around the axons (Olsen & Akirav, 2015). These processes wrap axons with several layers of myelin (Olsen & Akirav, 2015). The proteins and mRNA needed to synthesize the myelin sheath are delivered to these processes from the cell body of the oligodendrocyte (Olsen & Akirav, 2015). Some of these proteins are essential for adhesion between the neurons and the oligodendrocytes, and others are essential for stabilizing the myelin sheath (Olsen & Akirav, 2015).

### Models and Approaches to Study Demyelination and Remyelination

Currently, remyelination and demyelination are not well understood. There are still many unknowns about them, demyelinating diseases, and treatments. Some of these unknowns will be mentioned later. To study demyelination and remyelination further,

many models are used. These models can be classified as *in vitro*, *ex vivo*, or *in vivo* models. Some of these models are discussed in this section.

### *In Vitro Models*

*In vitro* models are models that use cells taken from humans or animals. These models can use OPCs, neurons, or both. Models that use these cells are discussed below.

### OPC Models

OPC models are those that use OPCs to study OPCs separately or to study them with neurons. That is, these models can consider OPCs the target of study and can be used to determine the molecules that influence the migration, proliferation, or differentiation of OPCs to understand remyelination better. On the other hand, OPCs can be used with neurons to study the mechanisms of demyelination and remyelination more by studying the interaction between neurons and OPCs during demyelination or remyelination.

In models that use OPCs, the OPCs can be obtained from multiple sources. OPCs can be obtained from the umbilical cord or fetal brain (Miller & Bai, 2007). Nonetheless, these sources raise ethical concerns. OPCs can also be obtained from the brains of rodents or through the usage of induced pluripotent stem cells (iPSCs) (Miller & Bai, 2007).

### Neurons in Culture

Models that use neurons study the effects of demyelination and remyelination on neurons when OPCs and other cells are present in culture. Neurons are not studied on their own because oligodendrocytes are the cells that are responsible for the

myelination of the axons of the neurons in the CNS. Without oligodendrocytes, myelination cannot be effectively studied.

Neurons can be natural or synthetic. Natural neurons are extracted from rats or mice (Miller & Bai, 2007). They can be extracted from the dorsal root ganglion or from the spinal cord (Miller & Bai, 2007). Neurons from the dorsal root ganglion are not CNS neurons, whereas MS and other demyelinating diseases affect the CNS (Miller & Bai, 2007). As a result, the data obtained using dorsal root ganglion neurons may not be applicable to these diseases. Spinal cord neurons, on the other hand, are CNS neurons. Regarding synthetic neurons, these can be made from glass microfiber, polystyrene, and other materials (Miller & Bai, 2007).

In sum, OPCs can be cultured on their own and, then, their role in demyelination and remyelination can be studied, or OPCs can be cultured with neurons to study their interaction during demyelination and remyelination. Nonetheless, culturing these cells is both time-consuming and expensive. As a result, in this project, the demyelination study that has been designed does not use an *in vitro* model.

### *Ex Vivo Models*

*Ex vivo* models are models that use tissue extracted from animals. The tissue can then be cultured in conditions similar to those that exist in the body (Miller & Bai, 2007). In these models, different tissue types can be used, such as cerebellum and spinal cord tissue (Miller & Bai, 2007).

To study demyelination and remyelination in these models; a demyelinating agent, a molecule that results in demyelination, is added to the tissue in the culture system

(Miller & Bai, 2007). Once demyelination occurs, OPCs differentiate into mature oligodendrocytes and remyelinate the axons of the neurons in the tissue (Miller & Bai, 2007). These models, thus, can be used to study demyelination and remyelination that occurs in response.

*Ex vivo* models are simple and result in quick demyelination and remyelination. As a result, an *ex vivo* demyelination study was designed and developed in this project.

### *In Vivo Models*

*In vivo* models are models that study animals. These models can use zebrafish or mammalian animals. Some of these models are discussed below.

#### *Zebrafish Models*

Zebrafish are transparent, allowing for imaging noninvasively and without needing to kill the animal (Miller & Bai, 2007). In these models, demyelination is induced by shining a laser light on the myelin, damaging the myelin (Miller & Bai, 2007). After demyelination, oligodendrocytes start to remyelinate the axons. To visualize the oligodendrocytes, transgenic zebrafish, in which oligodendrocytes have a fluorescent protein, have been developed (Miller & Bai, 2007). As a result, demyelination and remyelination can be observed in these models using confocal microscopy (Miller & Bai, 2007).

#### *Mammalian Animal Models*

Unlike zebrafish models, mammalian animals are killed so that histopathological studies and immunostaining can be conducted to detect the myelin (Miller & Bai, 2007). There

are multiple mammalian animal models, two of which are toxicity models and immune response models.

### ***Toxicity Models***

Toxicity models have two types: toxin-induced models and general toxicity models (Miller & Bai, 2007). Toxin-induced models involve injection of a toxin into a specific area in the animal to induce demyelination (Miller & Bai, 2007). For examples, lysophosphatidylcholine (LPC), or lysolecithin, can be injected into the animal (Miller & Bai, 2007). Regarding general toxicity models, these models involve the introduction of an agent through the diet (Miller & Bai, 2007). For example, cuprizone can be added to the diet of the animal to induce demyelination (Miller & Bai, 2007).

### ***Immune Response Models***

The major example of immune response models is the experimental autoimmune encephalomyelitis (EAE) model. In this model, T cells that target the myelin specifically are induced to activate, resulting in demyelination (Miller & Bai, 2007). This model is considered an immune response model because it involves T cells, which are part of the immune system. Further, this EAE model is the “gold standard model” for MS (Miller & Bai, 2007). EAE model is similar to MS in that demyelination occurs throughout the CNS in the model, but demyelination is more acute in the model than in MS (Miller & Bai, 2007). In addition, the model is expensive and complex because demyelination and remyelination occur at the same time, and it involves short studies, making it not useful for long term studies (Miller & Bai, 2007; Franklin, 2008).

In sum, zebrafish models are simpler *in vivo* models than toxicity and immune response models. However, *in vivo* study was not developed in this project because using animals requires approval and can be costly.

### Results of Studies of Demyelination and Remyelination

Using *in vitro*, *in vivo*, and *ex vivo* models different research studies on demyelination, remyelination, and demyelinating diseases have been conducted. These studies provided more data and information that can be used to develop treatments for demyelinating diseases. Some of the results of these studies concerning demyelination, and remyelination are discussed below.

#### *Demyelination*

Studies on demyelination revealed the cellular changes that occur in neurons as a result of demyelination. When demyelination occurs, the normal propagation of electrical signals through the axons is disrupted. Seeking the restoration of normal propagation, the number of NaV 1.2 channels and NaV 1.6 channels is increased (Franklin, 2008). This is done because electrical propagation through axons is mediated by sodium (Na<sup>+</sup>) channels. Hence, increasing the number of sodium Na<sup>+</sup> channels can preserve the propagation of the electrical signals. Nonetheless, overly increasing the number of these channels results in excess Na<sup>+</sup> in the neurons, resulting in loss of axons (Franklin, 2008). During demyelination, this over increase in Na<sup>+</sup> channels occurs (Franklin, 2008).

Another cellular change that occurs during demyelination is that mitochondria quantity increases in neurons (Franklin & Gallo, 2014). The number of mitochondria in neurons

is highest in demyelinated neurons, lower in remyelinated neurons, and lowest in normal neurons (Franklin & Gallo, 2014). Since mitochondria provides energy for cells, this result indicated that demyelinated neurons have a higher energy requirement than remyelinated or normal neurons (Franklin & Gallo, 2014).

### *Remyelination*

Studies on remyelination indicated morphological changes in neurons, promoters or remyelination, and inhibitors of remyelination. Regarding morphological changes in neurons, studies indicated that remyelinated neurons have thinner myelin sheath than normal neurons (Olsen & Akirav, 2015). Having a thin myelin sheath affects the propagation of electrical signals through neurons (Olsen & Akirav, 2015). Studies also indicated that remyelinated neurons have shorter internodes than normal neurons (Kremer, Kury, & Dutta, 2015).

Regarding promoters of remyelination, various molecules have been identified as promoters of remyelination. Some of these promoters are platelet-derived growth factor (PDGF), insulin-like growth factor 1 (IGF-1), and neuregulin (Nrg1) mitogen. PDGF has been shown to promote OPC proliferation and migration, which are steps of remyelination (Franklin, 2008). Nonetheless, PDGF inhibits full differentiation of OPC into mature oligodendrocytes (Franklin, 2008). Regarding IGF-1, this growth factor promotes neuronal proliferation and survival (Kuhl, De Keyser, De Vries, & Hoekstra, 2002). The activity of this growth factor is regulated by insulin-like growth factor binding proteins (IGFBPs) (Kuhl et al., 2002). In addition, Nrg1 mitogen plays a role in the survival of oligodendrocytes and results in increases myelin formation (Wang & Colognato, 2007).

Regarding inhibitors of remyelination, Notch receptor, polysialylated-neural cell adhesion molecule (PSA-NCAM), LRR and Ig domain-containing Nogo receptor-interacting protein (LINGO-1), and bone morphogenic protein (BMP) are inhibitors of remyelination (Lee et al., 2007). Notch receptors are located on OPCs and are activated by the ligand Jagged1 (Kremer et al., 2015). When activated, Notch receptor results in inhibition of the differentiation of oligodendrocytes (Kremer et al., 2015). Regarding PSA-NCAM, these molecules affect myelin formation (Charles et al., 2000). Further, LINGO-1 and BMP inhibit the differentiation of oligodendrocytes (Mi et al., 2007; Gallo & Armstrong, 2008).

#### Unknowns about Demyelination and Remyelination

Even though some aspects of remyelination and demyelination are known, such as those discussed above, other aspects are still unknown and need to be studied.

Studying these unknown aspects results in a better understanding of demyelination and remyelination, allowing for development of effective treatments for demyelinating diseases. Some of the unknowns about demyelination and remyelination are discussed below.

#### *Demyelination*

One of the unknown aspects of demyelination is regarding autoreactive T cells.

Autoreactive T cells play a role in demyelination, as mentioned above. These cells are specific to antigens of the body, such as MBP (Pette et al., 1990). The role of these cells in demyelinating diseases is not well understood. It is not clear whether these cells are the primary cause of demyelinating diseases or result in secondary effects in these

diseases (Singh & Sarma, 2016). Understanding the role of autoreactive T cells in the development and initiation of demyelinating diseases results in a better understanding of the nature of demyelinating diseases, allowing for the development of inhibitors of demyelinating diseases.

### *Remyelination*

The unknown aspects of remyelination are concerning the cellular changes that occur during remyelination and about the inhibitors of remyelination. As mentioned above, remyelination results in neurons with thinner myelin sheath than normal neurons (Olsen & Akirav, 2015). However, the mechanism for developing this thinner myelin sheath is unknown (Franklin, 2008). It is also not understood whether this thinner myelin is normally developed by oligodendrocytes that mature later in the life of a person or is an abnormal occurrence that results from the cellular environment of the disease (Olsen & Akirav, 2015). Another aspect that is unknown regarding the cellular changes during remyelination is about dystrophic neurons. As mentioned earlier, dystrophic neurons are rarely remyelinated (Franklin, 2008). It is not known whether when remyelination occurs, the dystrophy of the neurons is reversed (Franklin, 2008).

Regarding inhibitors of remyelination, unknown aspects exist about PSA-NCAM, LINGO-1, and BMP. The regulation of PSA-NCAM and LINGO-1 production is not well understood (Gallo & Armstrong, 2008). In addition, the mechanism of action of LINGO-1 is unclear (Bothwell, 2017). Regarding BMP, more studies about BMP's association with glial scar formation are needed (Gallo & Armstrong, 2008).

### Microscopic and Spectroscopic Methods Used to Detect the Myelin

To further study demyelination and remyelination and to shed light on the unknowns mentioned above, a microscopy method that can be used in these studies is needed. A microscopy method is needed because studies need to determine the changes that are occurring to the myelin and myelin levels during demyelination and remyelination. A microscopy method is also needed in studies that assess therapeutics because these studies need to determine whether remyelination is being stimulated, resulting in an increase in myelin levels. Hence, a microscopy method that can detect the myelin and visualize the myelin is needed.

Currently, various methods have been used to visualize or detect the myelin. These methods include fluorescence microscopy, multiphoton microscopy, spatially offset Raman spectroscopy (SORS), and near infrared (NIR) spectroscopy. However, these methods have different disadvantages, which are discussed below.

#### *Fluorescence Microscopy*

Fluorescence microscopy uses dyes of different colors to label structures and molecules in the cells. However, these dyes may affect the molecular functions of the cells and can experience bleaching (Lichtman & Conchello, 2005). Bleaching is when the dye stops emitting a color (Lichtman & Conchello, 2005). As a result, the molecule or structure can no longer be visualized under a microscopy. Because of this disadvantage, fluorescence microscopy may not be the best method for long term studies. Long term studies are useful when studying demyelination, remyelination, and assessing therapeutics.

### *Multiphoton Microscopy*

Multiphoton microscopy is an appealing method because it can allow for three-dimensional (3D) visualization of molecules and structures. Nonetheless, this method results in photobleaching, or bleaching (Ustione & Piston, 2011). In fact, high-order photobleaching can be observed in this type of microscopy, making it not suited for long term applications (Ustione & Piston, 2011).

### *Spatially Offset Raman Spectroscopy (SORS)*

SORS is a method that has a high penetration depth of light into tissue, allowing the visualization of molecules and cells deeper in tissues. Nonetheless, this method required more development. Currently, there is a need for the development of methodology to process and analyze the data obtained to allow for quantitative analysis of results (Rae et al., 2014).

### *Near Infrared (NIR) Spectroscopy*

NIR spectroscopy is a well-known spectroscopy method that is used in various fields. Nonetheless, this method has disadvantages. NIR spectroscopy is not selective, and it requires calibration models, which are often difficult to develop or obtain (Blanco & Villarroya, 2002). Since studies of demyelinating and remyelination require selectivity and specificity for myelin, this method is not the best option.

In sum, the methods mentioned above result in bleaching, require development of an analysis method, or are not selective and need calibration. A method that has been used to visualize the myelin and does not have these disadvantages is coherent anti-Stokes Raman spectroscopy (CARS). CARS microscopy's bleaching can be attenuated

or lowered by adjusting the wavelength of the lasers used, and CARS has analysis methods and high specificity and selectivity for molecules, such as the lipids in the myelin sheath. As a result, CARS can be used in demyelination and remyelination studies. CARS allows visualizing the myelin, resulting in determination of the changes that are occurring to the myelin in studies and allowing for assessment of therapeutic agents that increase the myelin levels.

### Project Overview

In this project, the necessary steps needed to allow for usage of CARS to study demyelination and remyelination are taken. Using CARS to study demyelination or remyelination proves its usefulness in demyelination and remyelination studies and shows its ability to detect changing levels of myelin. Detecting changing levels of myelin is important in the assessment of therapeutic agents because these agents change the levels of myelin by increasing them.

Specifically, in this project, the CARS microscope was used to image engineered adipose tissue because it contains lipids, and myelin consist primarily of lipids. In addition, an image processing protocol has been developed to allow for the analysis of the acquired images. A mini incubation chamber, which fits on the stage of the microscope, was also designed and built. This incubation chamber allows for long term studied using the CARS microscope. Additionally, a procedure for a demyelination study using an *ex vivo* model has been designed. Overall, this project shows that CARS microscope can be used to image lipids, which are a major constituent of myelin. The project also shows that the images can be analyzed, and the project paves the road for

a future demyelination study through the building of a mini incubation chamber and the design of a demyelination study.

## Methods

### *Imaging of Engineered Adipose Tissue*

Engineered adipose tissue was provided by Dr. Evangelica Bellas from the Bioengineering department. Three samples of each culture were provided: oleic acid, palmitic acid, and control. The control did not contain oleic acid or palmitic acid in the culturing media. Before taking CARS images, the microscope was used to obtain 2-photon images of any of the samples to test the microscope. The wavelength of the laser was 730 nm. These images were obtained by me, Shahriar, or other undergraduate students in Dr. Patil's lab.

Each day for three days, Shahriar, the master's student, obtained a CARS Z stack from each sample by locating the depth range where lipid droplets could be seen. Each z stack took around 40 minutes. During imaging, the lasers of the CARS microscope were set at 801 nm and 1040 nm.

### *Image Analysis in ImageJ*

The Z stack images were analyzed using Fiji, a version of ImageJ (a free NIH software). ImageJ was used to process the images and enhance their contrast, quantify the number of lipid droplets, and measure their surface area and volume. The following tools were used: Enhance Contrast, Subtract Background, Brightness/Contrast, 3D Objects Counter, Z Project, Lookup Tables, and Merge Channels, in addition to other common tools (a description of these tools is provided in the Results section).

### *Design and Construction of a Mini Incubation Chamber*

The mini incubation chamber controls humidity, temperature, and CO<sub>2</sub> levels (see Figure 1 below). To control humidity, Arduino Uno opens a strip heater to heat water in a water reservoir based on the readings from the humidity sensor DHT22 (see Figure 2). If humidity is below 80%, Arduino Uno opens the strip heater to heat the water to get more vapor. If the humidity is above 90%, Arduino Uno closes the heater. Between the threshold of 80% and the setpoint of 90%, the heater is opened for 2 seconds and closed for 2 seconds. 90% was chosen as the setpoint, which should be maintained, because the CO<sub>2</sub> sensor tolerates up to 95% non-condensing relative humidity (RH).

To control temperature, Arduino Uno opens or closes two strip heaters attached to an aluminum ring, on which the petri dish is placed, based on the readings from a thermocouple attached to the aluminum ring (see Figures 1 and 3). If the temperature is below 40 degrees Celsius, Arduino Uno opens the strip heaters. If the temperature is above 42 degrees Celsius, Arduino Uno closes the heaters. Between the threshold of 40 degrees Celsius and the setpoint of 42 degrees Celsius, the heater is opened for 2 seconds and closed for 2 seconds. 42 degrees Celsius was chosen as the setpoint, which should be maintained, because testing with water indicated that when the temperature of the aluminum ring is 42 degrees Celsius, the temperature of the water in the petri dish is 37 degrees Celsius as measured by a temperature sensor placed inside the petri dish. 37 degrees Celsius is required for optimal growth of cells.

To control CO<sub>2</sub> levels, Arduino Uno opens or closes a gas valve based on the readings of a 20% CO<sub>2</sub> sensor (see Figure 4). If CO<sub>2</sub> levels are less than 4.5%, Arduino Uno opens the gas valve to release more CO<sub>2</sub> into the incubation chamber. If CO<sub>2</sub> levels

are above 5%, the gas valve is closed. Between the threshold of 4.5% and the setpoint of 5%, the heater is opened for 2 seconds and closed for 2 seconds. The setpoint was chosen to be 5% because culturing cells or tissue requires 5% CO<sub>2</sub>.

The body of the chamber and the water reservoir were 3D printed. The material used to 3D print the water reservoir and its lid has a melting point of around 120degrees Celsius, meaning it will not melt upon heating the water reservoir.

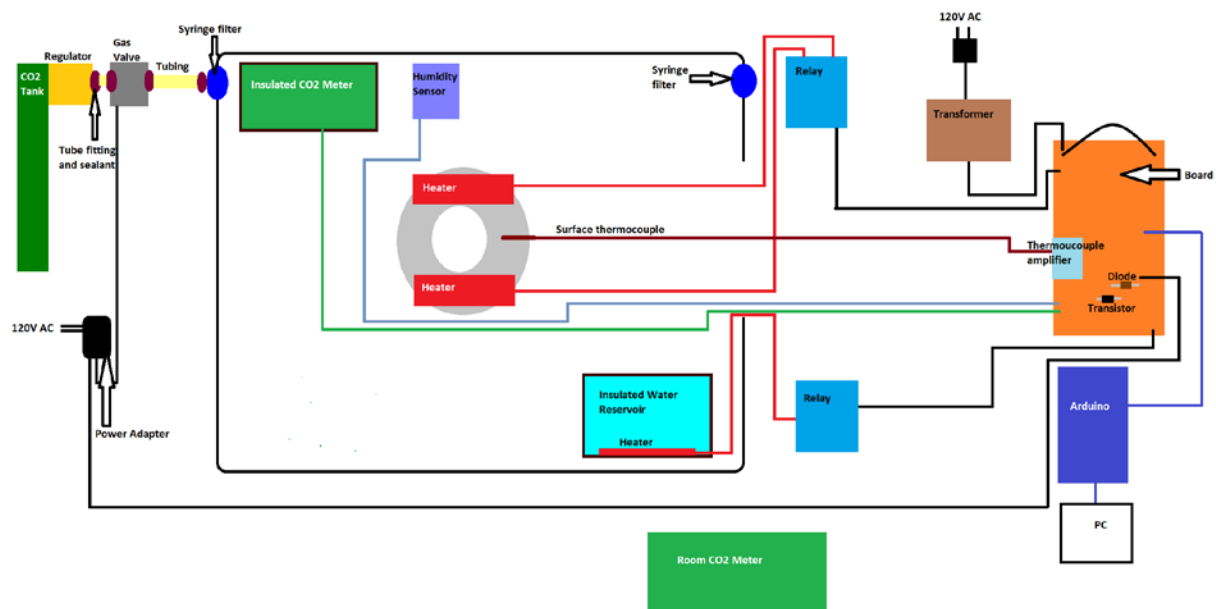


**Figure 1.** This figure shows the full design of the incubation chamber with the circuitry.

Note: The gas valve is controlled by a relay in the final design, not by a transistor and a diode as shown in this design.

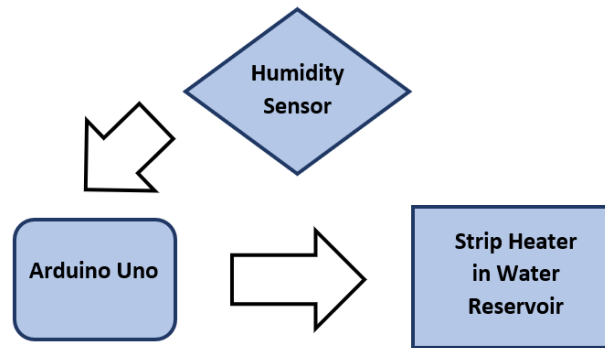


**Figure 2.** This figure shows the feedback control for controlling humidity levels in the incubation chamber. A humidity sensor provides data to Arduino Uno. Based on the data, Arduino Uno opens or closes a heater in a water reservoir. Heating the water produces vapor that humidifies the chamber.

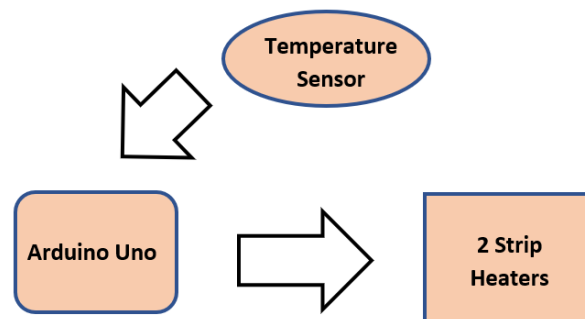


**Figure 3.** This figure shows the feedback control for controlling temperature in the incubation chamber. A temperature sensor, or thermocouple, measures the temperature of an aluminum ring, on which a petri dish is placed. The temperature readings are sent to Arduino Uno, and Arduino Uno opens or closes two strip heaters attached to the aluminum ring based on the readings.

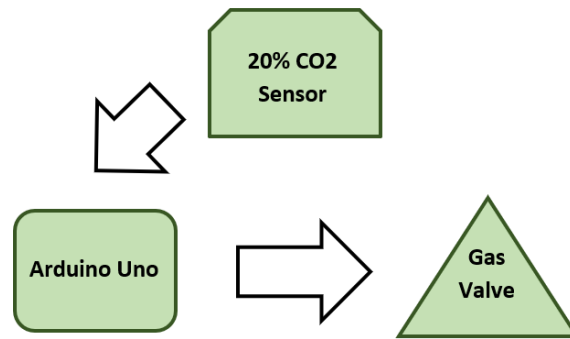


**Figure 4.** This figure shows the feedback control for controlling CO<sub>2</sub> levels in the incubation chamber. A CO<sub>2</sub> sensor measures CO<sub>2</sub> levels in the chamber and sends the data to Arduino Uno. Arduino Uno opens or closes a gas valve, which is attached to a gas tank (5% CO<sub>2</sub> with 95% Air).

#### *Developing a Procedure for Demyelination*

Previous demyelination studies that used the toxin lysophosphatidylcholine, or lysolecithin, were read. Also, to develop the imaging procedure for demyelination, studies that used CARS to image brain tissue were read.

#### Results

##### *Imaging of Engineered Adipose Tissue*

When taking 2-photon images of the samples, sometimes the lipid droplets did not appear. Changing the power level of the laser beam and the wavelength of the laser resulted in the appearance of the lipid droplets on the microscope.

CARS Z stack images were acquired from the samples. All of the control and oleic acid samples were imaged on the three days. The three days were not consecutive. Images were taken on two consecutive days, then a day was skipped. Regarding the palmitic

acid samples, only one sample was imaged on the first day, and only two samples were imaged on the second day. However, on the third day, all palmitic acid samples were imaged.

During 2-photon and CARS imaging, the power level of the laser beams had to be adjusted to enhance the contrast of the images acquired. Nonetheless, the contrast of the images remained poor in some of the images (see figure 5 below). In addition, imaging was time consuming. Each Z stacks required 40 min, excluding the time required to put the objective lens in focus and to adjust the power level of the laser beams.



**Figure 5.** This figure shows an image with poor contrast from the CARS Z stack images of a control sample acquired on the second day. The grey round objects that appear in the image are adipocytes and lipid droplets.

#### *Image Analysis in ImageJ*

The CARS Z stack images were processed and analyzed using Fiji. The developed image processing protocol consisted of using the following tools: Enhance Contrast,

Subtract Background, Brightness/Contrast, 3D Objects Counter, Z Project, Lookup Tables, and Merge Channels, in addition to common tools. The Enhance Contrast tool makes the pixel value range in an image equal to the maximum range allowed for the image type (Ferreira & Rasband, 2012). For example, an 8-bit grey scale image has a pixel value range from 0 to 255 (Ferreira & Rasband, 2012). An image with a low contrast similar to the “Original Image” in Figure 6 may have a pixel value range from 50 to 150. Using the Enhance Contrast tools changes the range of pixel values from 50 to 150 to become 0 to 255, making the image clearer. When the Enhance Contrast tool was applied to the Z stack images, the “Original Image” in Figure 6 became clearer.

The Subtract Background tool uses a “rolling ball” algorithm (BackgroundSubtractor.java, 2008). In this algorithm, the 2D image becomes a 3D image by considering its pixel values as the height at each location in the image (BackgroundSubtractor.java, 2008). Then, a ball rolls on the underside of the formed 3D surface (BackgroundSubtractor.java, 2008). The volume that the ball covers is considered the background and is subtracted. The Subtract Background tool can use sliding paraboloids instead of a ball. The developed procedure uses sliding paraboloid because testing indicated that it results in clearer images. When the Subtract Background tool was applied to the Z stack images, the “Enhanced Contrast” image in Figure 6 became a little darker because the background was subtracted, becoming black.

The Brightness/Contrast tool allows the user to adjust the brightness and contrast of an image. This tool was used to make the background as dark as possible and to keep only the white adipocytes and lipid droplets. When applied to the Z stack images, the

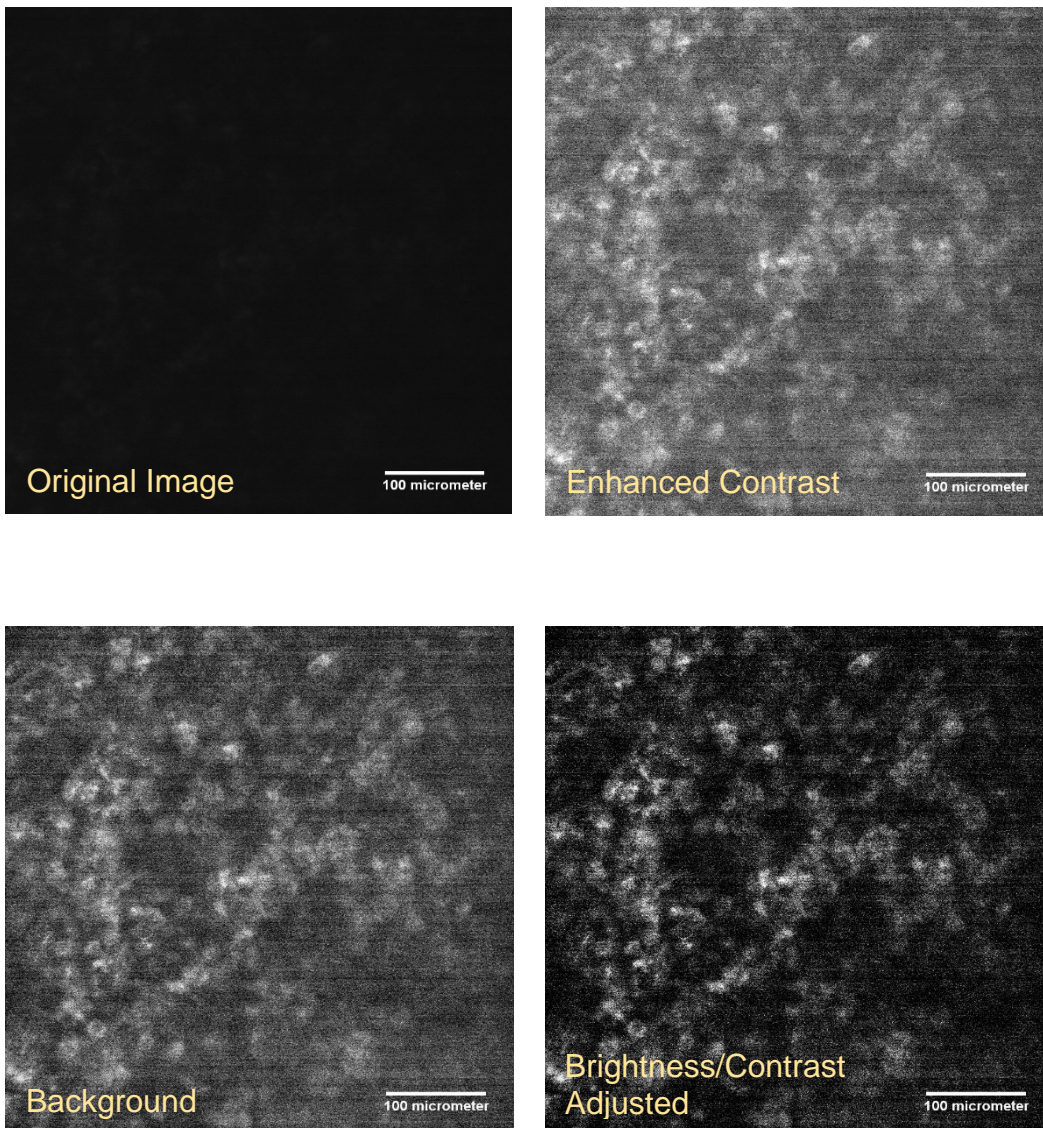
“Background Subtracted” image obtained better contrast because the background became darker than before.

The 3D Objects Counter tool quantifies 3D objects and measures their surface area, volume, and other parameters (ImageJ, 2017). This tool requires choosing a threshold. The “Threshold for 3D Objects Counter” image in Figure 6 shows the threshold set when processing the Z stack images. Choosing the threshold highlights the “objects” in the image. Everything that is not highlighted is considered background. When this threshold is applied to the Z stack images, a Z stack with the objects highlighted in each image and data of the size and volume of the objects are provided (see Figure 6). The “3D Objects Counter Output” 2D image is formed by flattening the output Z stack by using the Z Project tool (Ferreira & Rasband, 2012).

The Z stack images of the sample after processing are colored using the Lookup Tables tool. This tool can color an image by assigning it matching values (Ferreira & Rasband, 2012). The Lookup Tables have the red, green, and blue values that match or coincide with grey values, and the tool uses these values to color an image (Ferreira & Rasband, 2012). The “Colored Z Projection of Z Stack” image in Figure 6 shows the colored flattened Z stack.

The Merge Channels tool merges multiple images into a multi-composite image (Ferreira & Rasband, 2012). This tool was used to merge the “3D Objects Counter Output” image with the “Colored Z Projection of Z Stack” image to provide an image that shows the lipid droplets in a yellow color on top of the adipocytes.

The data provided by the 3D objects counter tool was used to make histograms of the surface area and volume of the lipid droplets (Figures 7 and 8). In both of these histograms the data has a wide range. The histograms also show that there are many droplets with small surface area and volume.



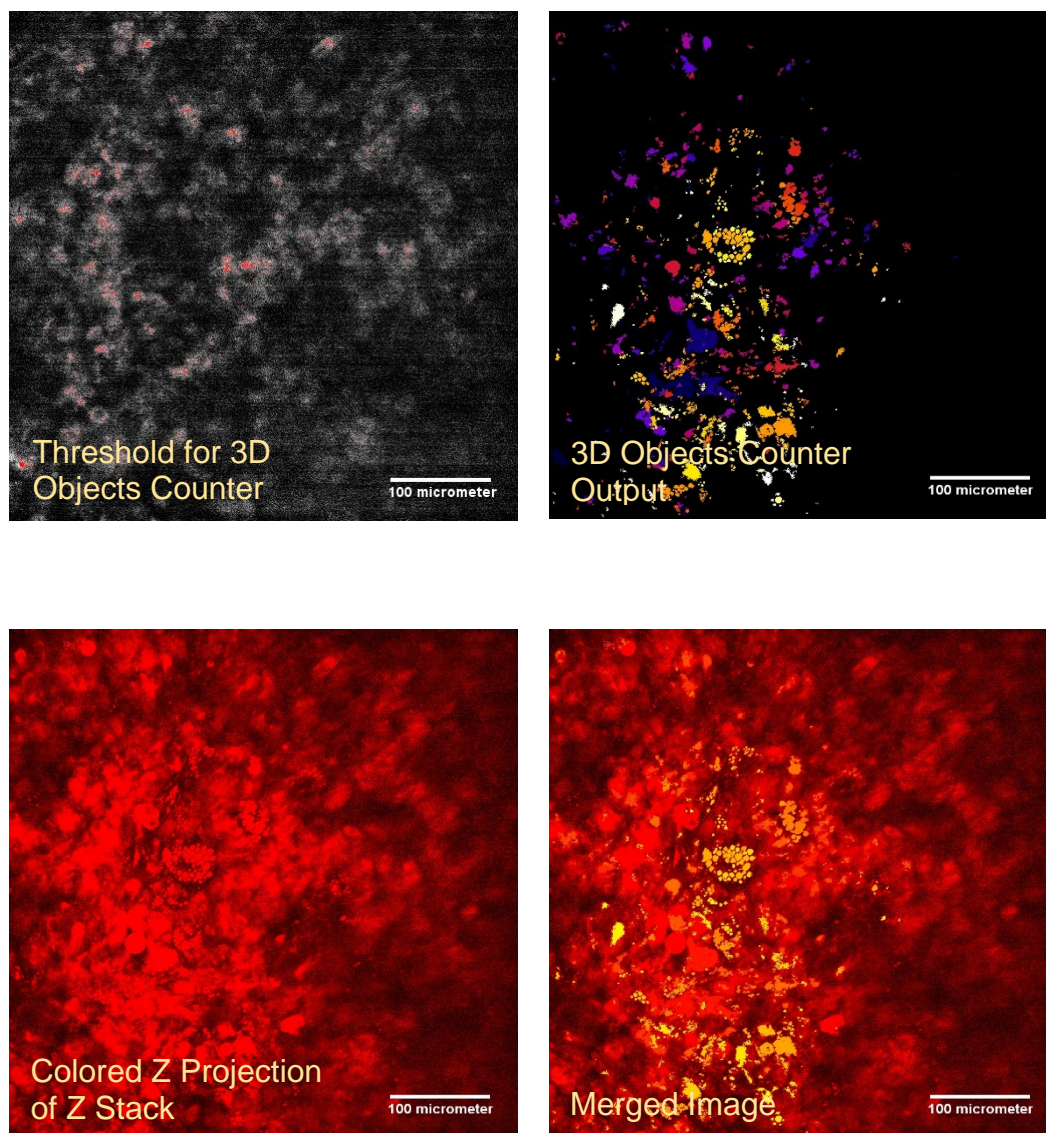


**Figure 6.** This figure shows the results of the steps developed image processing protocol.

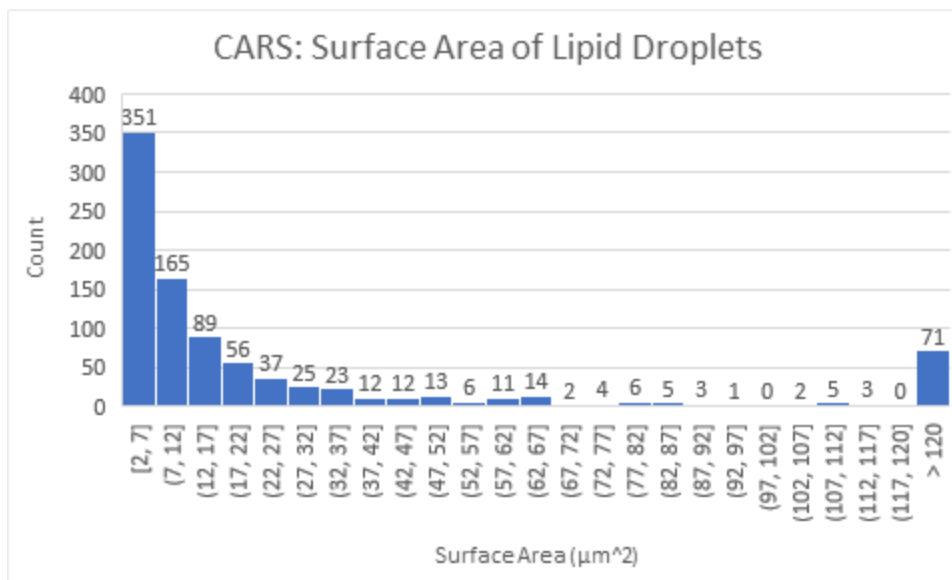


**Figure 7.** This figure shows a histogram of the surface area of the lipid droplets. The data used to make the histogram was a part of the output of the 3D Objects Counter tool.

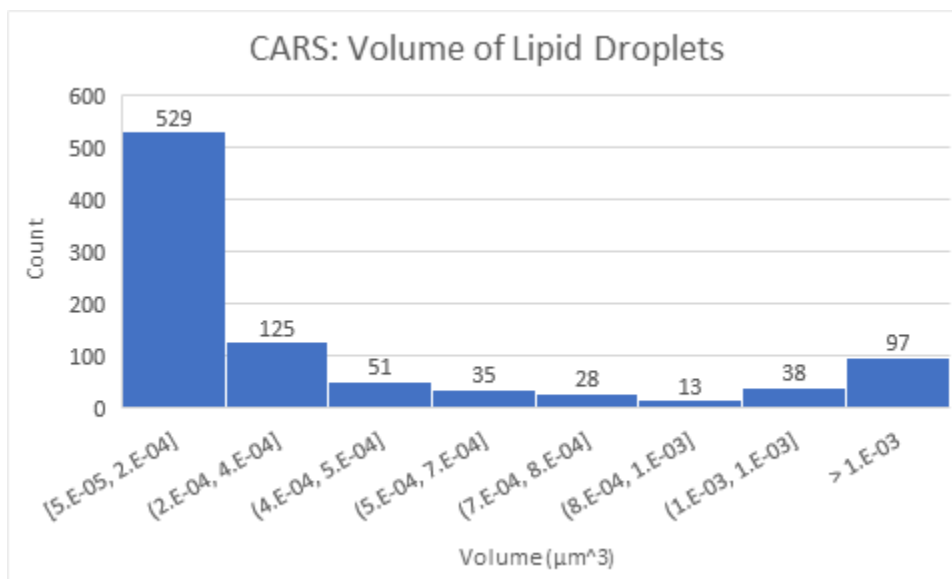


**Figure 8.** This figure shows a histogram of the volume of the lipid droplets.

### *Construction of a Mini Incubation Chamber*

The incubation chamber was designed to hold aluminum ring with heaters and a temperature sensor, CO<sub>2</sub> sensor, humidity sensor, thermally insulated water reservoir with a heater, and foam to avoid gas leakage. The chamber and its lid can be seen in Figure 9. The chamber was also designed to have a gas inlet and a gas exit and a hole for electrical wiring. It also was designed to fit the stage of the microscope (see Figure 10).

Figure 11 shows the setup for humidity control testing. A water bottle was heated because the designed water reservoir, which is shown in Figure 12, was not 3D printed. During humidity control testing, RH reached 80% at approximately 2 min, which was the threshold, and kept increasing (see Figure 13). RH decreased at the end of testing because the lid of the chamber was removed.

Figure 14 shows the setup for temperature control testing. Temperature of the water in the petri dish reached 37 degrees Celsius after approximately 7 min of the beginning of the testing (see Figure 15). There was only a 0.25 degrees Celsius increase from the desired 37 degrees Celsius.

The code for CO<sub>2</sub> control was tested, and it worked properly. Nonetheless, actual testing with gas was not performed because the gas tank was not ordered.



**Figure 9.** This figure shows the incubation chamber (top) and the lid of the incubation chamber (bottom).



**Figure 10.** This figure shows the stage of the microscope (left) and the bottom side of the incubation chamber (right). The incubation chamber fits the dimensions of the stage.



**Figure 11.** This figure shows the setup for humidity control testing. The water bottle contains water, and there is a heater wrapped around its exterior to heat the water to produce steam. The white cubic object is the humidity sensor. The aluminum ring on the bottom of the chamber is attached to two heaters and to a temperature sensor covered with electrical tape.

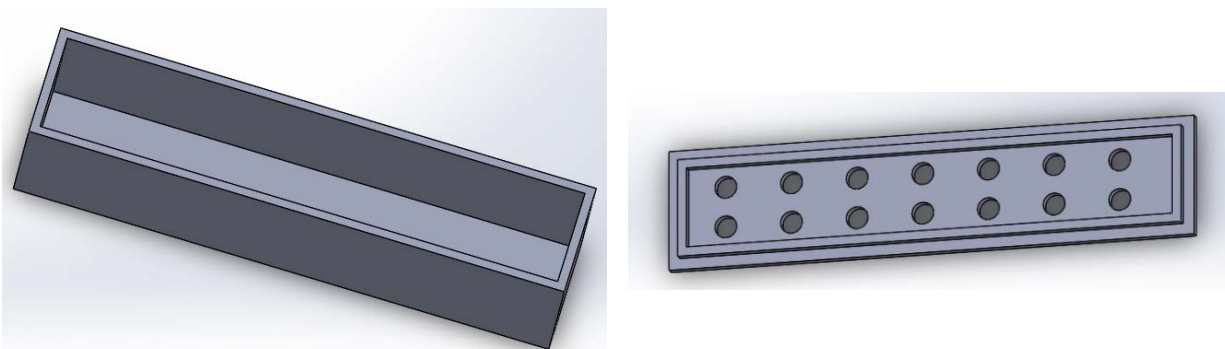


**Figure 12.** This figure shows the water reservoir (left) and its lid (right). The lid has holes to minimize the amount of vapor that is released into the incubation chamber to

make control of humidity easier and prevent an overshoot of humidity over the 90% setpoint.

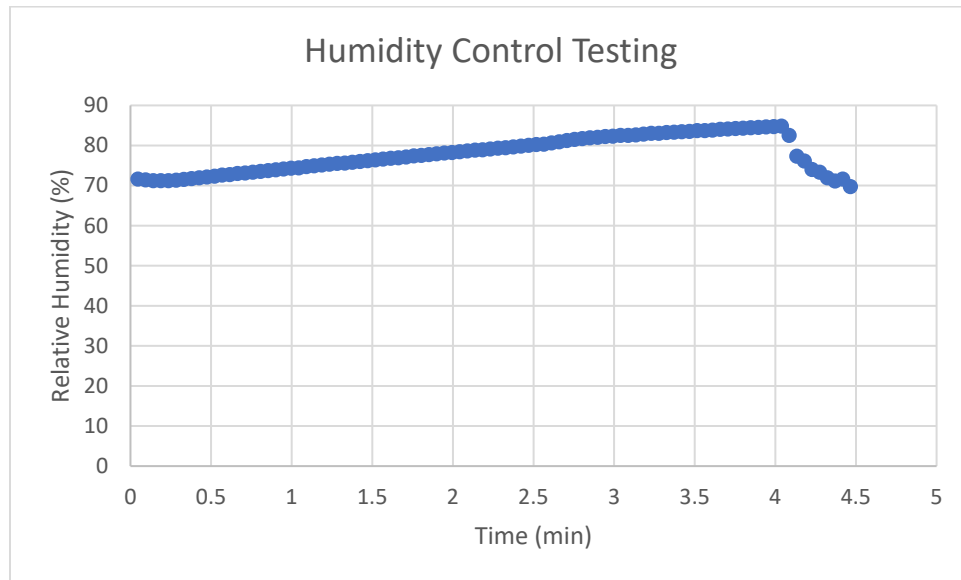


**Figure 13.** This plot shows RH during relative humidity control testing. Humidity reached the threshold of 80% at approximately 2 min and kept increasing until the lid of the incubation chamber was opened, resulting in a drop in humidity.

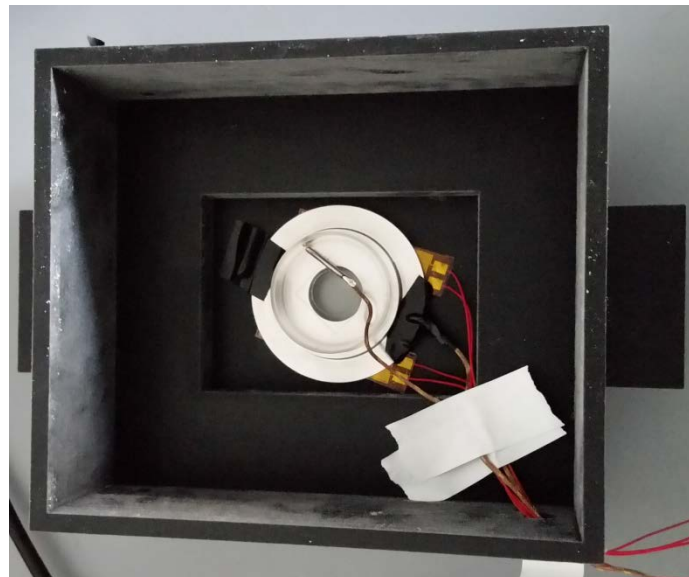


**Figure 14.** This figure shows the setup for temperature control testing. A petri dish (not shown) was placed on the aluminum ring, and a temperature sensor (probe with silver tip) was placed inside the water in the petri dish. The aluminum ring is attached to two heaters and a temperature sensor covered with electrical tape.

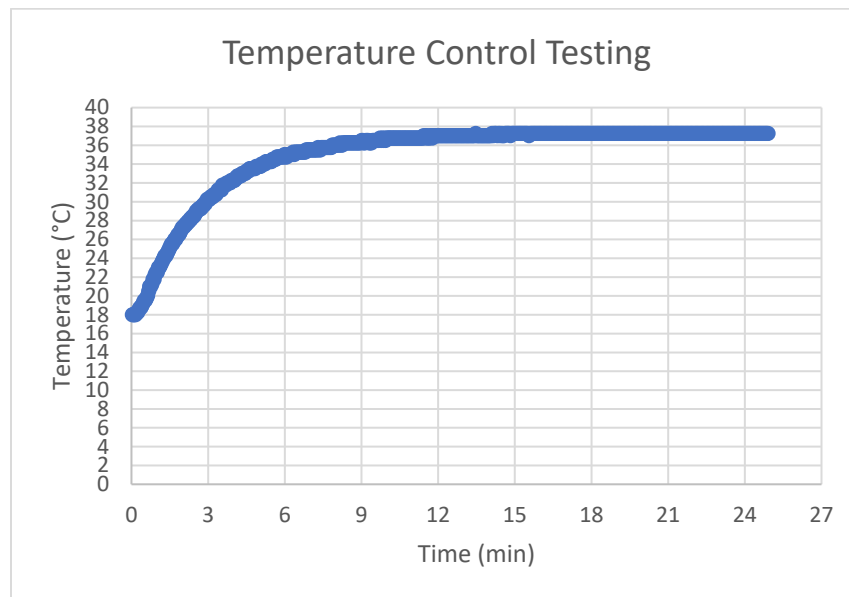


**Figure 15.** This plot shows temperature of the water in the petri dish during temperature control testing. Temperature reached the desired temperature of 37 degrees Celsius at approximately 7 min, and there was only an increase of 0.25 degrees Celsius over the desired 37 degrees Celsius.

### *Developing a Procedure for Demyelination*

Studies that studied demyelination induced by the toxin lysolecithin differed in the type of animal studied, age of animal, type of tissue, and method of culture after demyelination. However, the procedures by Birgbauer, Rao, and Webb (2004) and by Cho et al. (2010) will be used because of their clarity and similarity with other studies. Day 10 or Day 6 postnatal Sprague-Dawley rats will be used, specifically cerebellum or

spinal cord tissue sliced will be used. The slices will be cultured for 7 days, in which the media will be changed twice. After the seventh day, 0.5 mg/mL of lysolecithin (from Sigma-Aldrich) will be added to the fresh media, and the slices will be incubated in the mini incubation chamber for 15-17 hours, during which long-term imaging will be performed (Birgbauer et al., 2004; Cho et al., 2010). After incubation, the media will be replaced with fresh media (Birgbauer et al., 2004; Cho et al., 2010).

For the imaging protocol, the parameters in the procedure of Meyer et al. (2011) will be followed. The Stokes laser will be set at 830 nm, and the pump laser will be tuned between 500 to 800 nm. The laser power at the sample will be around 50 mW. These parameters were used because they allow imaging a wide spectrum of wavenumbers.

## Discussion

### *Imaging of Engineered Adipose Tissue*

As mentioned in the Results section, the Z stack images had poor contrast. To enhance contrast the background can be subtracted during imaging of samples by the software used for imaging, which is ThorImageLS. In addition, imaging was time consuming because each stack needs around 40 min to be collected. To reduce this amount of time, a quicker computer and a quicker microscope scanning camera should be used.

### *Image Analysis in ImageJ*

The Results indicated that a large number of lipid droplets had small surface area and volume. This may be caused by incorrect quantification of lipid droplets. Because the contrast in the images is poor, a single lipid droplet will appear as if it has gaps. As a

result, 3D Objects Counter quantifies the disjointed lipid droplet as multiple smaller droplets.

#### *Construction of a Mini Incubation Chamber*

Humidity control testing indicated that humidity steadily increases after reaching the 80% threshold, which will result in going over the setpoint of 90%. As a result, the code for humidity control should be modified so that the heater opens before 85% and closes above 85%. This way water will keep producing vapor after reaching 85% because it is still warm, reaching 90%. Nonetheless, once humidity reaches 90%, water would have begun to cool down.

Temperature control testing resulted in maintaining the temperature of water at 37 degrees Celsius after 7 min of the beginning of the test. This 7 min will be less when using samples that have been brought from an incubator that already maintains their temperature at 37 degrees Celsius. In addition, testing with culture media should be conducted to verify the threshold and setpoint chosen.

The code for CO<sub>2</sub> control works properly. However, the gas valve has a low flow rate. If testing with a gas tank indicates that this is an issue, another gas valve will be used.

#### *Developing a Procedure for Demyelination*

The procedure for inducing demyelination is straightforward. However, it requires 7 days of culturing (Birgbauer et al., 2004). To reduce this amount of time, older animals may be used because older animals are already myelinated, eliminating the need for 7 days of culture to allow for myelination of the tissue (Cho et al., 2010).

## Conclusion

The built microscope works properly, but the contrast of the images acquired needs to be increased. In addition, the developed image analysis protocol provides the needed data, but its data is affected by the contrast of the acquired images, increasing the need for better images. In addition, the incubation chamber can maintain temperature at 37 degrees Celsius. Humidity control testing needs to be finished and CO2 control needs to be tested using a gas tank. Further, the procedure for imaging brain tissue during demyelination has been developed.

## Acknowledgements

This project was funded by Creative Arts, Research, and Scholarship (CARAS) grant.

Engineered adipose tissue samples from Evangelica Bellas and her graduate student Golnaz Anvari are appreciated. The author thanks Shahriar Rashvand for building the microscope. The author also thanks Yonis Hakim for his help in designing the incubation chamber and assistance in the construction of the microscope; Brandon Harrison for his help in coordinating with the members involved; Nina Mucciolo, Kavya Sreeram, and Jerry So for their help in imaging and image processing; and Helen Freitas for her help in ordering the materials needed.

## References

- Alberts, B., Johnson, A., Lewis, J., Walter, P., Raff, M., & Roberts, K. (2002). Molecular Biology of the Cell 4th Edition: International Student Edition.
- Background Subtractor.java (2008). Retrieved from

<https://imagej.nih.gov/ij/developer/source/ij/plugin/filter/BackgroundSubtractor.java.html>

- Birgbauer, E., Rao, T. S., & Webb, M. (2004). Lysolecithin induces demyelination in vitro in a cerebellar slice culture system. *Journal of neuroscience research*, 78(2), 157-166.
- Blanco, M., & Villarroya, I. N. I. R. (2002). NIR spectroscopy: a rapid-response analytical tool. *TrAC Trends in Analytical Chemistry*, 21(4), 240-250.
- Bothwell, M. (2017). Mechanisms and medicines for remyelination. *Annual review of medicine*, 68, 431-443.
- Charles, P., Hernandez, M. P., Stankoff, B., Aigrot, M. S., Colin, C., Rougon, G., ... & Lubetzki, C. (2000). Negative regulation of central nervous system myelination by polysialylated-neural cell adhesion molecule. *Proceedings of the National Academy of Sciences*, 97(13), 7585-7590.
- Cho, Y. K., Kim, G., Park, S., Sim, J. H., Won, Y. J., Hwang, C. H., ... & Hong, H. N. (2012). Erythropoietin promotes oligodendrogenesis and myelin repair following lysolecithin-induced injury in spinal cord slice culture. *Biochemical and biophysical research communications*, 417(2), 753-759.
- Ferreira, Tiago & Rasband, Wayne. (2012). ImageJ user guide. Retrieved from <https://imagej.nih.gov/ij/docs/guide/146.html>
- Franklin, R. J. (2008). Remyelination in the CNS: from biology to therapy. *Nature Reviews Neuroscience*, 9(11), 839.

- Franklin, R. J., & Gallo, V. (2014). The translational biology of remyelination: past present, and future. *Glia*, 62(11), 1905-1915.
- Gallo, V., & Armstrong, R. C. (2008). Myelin repair strategies: a cellular view. *Current opinion in neurology*, 21(3), 278-83.
- Goldschmidt, T., Antel, J., König, F. B., Brück, W., & Kuhlmann, T. (2009). Remyelination capacity of the MS brain decreases with disease chronicity. *Neurology*, 72(22), 1914-1921.
- ImageJ. (2017). 3D objects counter. Retrieved from [https://imagej.net/3D\\_Objects\\_Counter](https://imagej.net/3D_Objects_Counter)
- Kremer, D., Küry, P., & Dutta, R. (2015). Promoting remyelination in multiple sclerosis: current drugs and future prospects. *Multiple Sclerosis Journal*, 21(5), 541-549.
- Kühl, N. M., De Keyser, J., De Vries, H., & Hoekstra, D. (2002). Insulin-like growth factor binding proteins-1 and-2 differentially inhibit rat oligodendrocyte precursor cell survival and differentiation in vitro. *Journal of neuroscience research*, 69(2), 207-216.
- Lee, X., Yang, Z., Shao, Z., Rosenberg, S. S., Levesque, M., Pepinsky, R. B., ... & Mi, S. (2007). NGF regulates the expression of axonal LINGO-1 to inhibit oligodendrocyte differentiation and myelination. *Journal of Neuroscience*, 27(1), 220-225.
- Lichtman, J. W., & Conchello, J. A. (2005). Fluorescence microscopy. *Nature methods*, 2(12), 910.

- Meyer, T., Bergner, N., Krafft, C., Akimov, D., Dietzek, B., Popp, J., ... & Kalff, R. (2011). Nonlinear microscopy, infrared, and Raman microspectroscopy for brain tumor analysis. *Journal of biomedical optics*, 16(2), 021113.
- Miller, R. H., & Bai, L. (2007). Cellular approaches for stimulating CNS remyelination.
- Mi, S., Hu, B., Hahm, K., Luo, Y., Hui, E. S. K., Yuan, Q., ... & Guo, J. (2007). LINGO-1 antagonist promotes spinal cord remyelination and axonal integrity in MOG-induced experimental autoimmune encephalomyelitis. *Nature medicine*, 13(10), 1228.
- Olsen, J. A., & Akirav, E. M. (2015). Remyelination in multiple sclerosis: cellular mechanisms and novel therapeutic approaches. *Journal of neuroscience research*, 93(5), 687-696.
- Pette, M., Fujita, K., Wilkinson, D., Altmann, D. M., Trowsdale, J., Giegerich, G., ... & Wekerle, H. (1990). Myelin autoreactivity in multiple sclerosis: recognition of myelin basic protein in the context of HLA-DR2 products by T lymphocytes of multiple-sclerosis patients and healthy donors. *Proceedings of the National Academy of Sciences*, 87(20), 7968-7972.
- Rae, A., Stosch, R., Klapetek, P., Walker, A. R. H., & Roy, D. (2014). State of the art Raman techniques for biological applications. *Methods*, 68(2), 338-347.
- Singh, M., & Sarma, J. D. (2016). Demyelinating Diseases and Neuroinflammation. In *Inflammation: the Common Link in Brain Pathologies* (pp. 139-170). Springer, Singapore.

Ustione, A., & Piston, D. W. (2011). A simple introduction to multiphoton microscopy.

*Journal of microscopy*, 243(3), 221-226.

Wang, Z., & Colognato, H. (2007). Contrasting effects of mitogenic growth factors on

myelination in neuron–oligodendrocyte co-cultures. *Glia*, 55(5), 537-545.